environments

Article

Morphological Alterations and Oxidative Stress Induction in *Danio rerio* Liver After Short-Term Exposure to the Strobilurin Fungicide Dimoxystrobin

Rachele Macirella [1,†], Abdalmoiz I. M. Ahmed [1,†], Federica Talarico [1,2], Naouel Gharbi [3], Marcello Mezzasalma [1] and Elvira Brunelli [1,*]

[1] Department of Biology, Ecology and Earth Science (DiBEST), University of Calabria, Via P. Bucci 4/B, 87036 Rende, Italy; rachele.macirella@unical.it (R.M.); abdalmoiz.ahmed@unical.it (A.I.M.A.); federica.talarico@unical.it (F.T.); marcello.mezzasalma@unical.it (M.M.)
[2] Natural History Museum and Botanical Garden, University of Calabria, 87036 Rende, Italy
[3] Fish Biology and Aquaculture Group, Ocean and Environment Department, NORCE Norwegian Research Center, 5006 Bergen, Norway; nagh@norceresearch.no
* Correspondence: elvira.brunelli@unical.it
† These authors contributed equally to this work.

Abstract: Unlike many other fungicides, strobilurins are applied several times during the growing season for prophylactic purposes, thus heightening the risk of environmental contamination. In the EU, the dimoxystrobin approval period lasted for 17 years. It has been classified as moderately toxic to birds and highly toxic to earthworms, and it is suspected to be carcinogenic to humans. However, it is still commercialized in several countries. The effects of dimoxystrobin are still largely underexplored, with only three studies reporting sublethal alterations in fish. Here, we evaluated for the first time the effects of dimoxystrobin on zebrafish liver after short-term exposure (96 h) to two sublethal and environmentally relevant concentrations (6.56 and 13.13 µg/L), providing evidence of morphological, functional, and ultrastructural modifications. We revealed severe alterations encompassing three reaction patterns: circulatory disturbance, regressive and progressive changes, which also showed a dose-dependent trend. Furthermore, we revealed that dimoxystrobin induced a significant increase in lipid content, a decrease in glycogen granules and affected the defensive response against oxidative stress through a significant downregulation of SOD and CAT. The information presented here demonstrates that the hazardous properties of dimoxystrobin may result from several pathological events involving multiple targets. Our results also emphasize the importance of the combined use of morphological, ultrastructural and functional investigation in ecotoxicological studies.

Keywords: pesticides; hepatotoxicity; histological biomarkers; ultrastructure; molecular biomarkers; glycogen granules; lipid content; SOD; CAT

check for updates

Citation: Macirella, R.; Ahmed, A.I.M.; Talarico, F.; Gharbi, N.; Mezzasalma, M.; Brunelli, E. Morphological Alterations and Oxidative Stress Induction in *Danio rerio* Liver After Short-Term Exposure to the Strobilurin Fungicide Dimoxystrobin. *Environments* **2024**, *11*, 282. https://doi.org/10.3390/environments11120282

Academic Editors: Ge Zhang and John D. Stark

Received: 4 November 2024
Revised: 2 December 2024
Accepted: 5 December 2024
Published: 7 December 2024

Copyright: © 2024 by the authors. Licensee MDPI, Basel, Switzerland. This article is an open access article distributed under the terms and conditions of the Creative Commons Attribution (CC BY) license (https://creativecommons.org/licenses/by/4.0/).

1. Introduction

To meet the needs of an ever-increasing global population, the productivity growth rate in agriculture tripled between 1960 and 2015, thus exceeding that of many other sectors and food demand will increase by a further 70% in 2050 [1,2]. Such enormous production growth requires overexploitation of the land and a proportional increase in the use of agrochemicals [3,4].

According to data from Eurostat [5], fungicides are the pesticide group with the highest sales volumes in the EU, and their use is not expected to decrease in the next few years. Since their approval for use on crops in the EU and USA in 1996 and 1997, strobilurins have quickly become a leading choice in the fungicide market [6,7]. Once introduced into the environment, they can reach aquatic systems through the drainage flow and runoff from the soil [7,8], and they are found in both surface and groundwater worldwide [9].

Strobilurins belong to quinone outside inhibitor (QoI) fungicides and exert their antifungal action by impairing electron transfer in the mitochondrial respiratory chain, ultimately blocking ATP production [10]. Given this non-specific mode of action, strobilurin fungicides can exert their harmful effects on non-target organisms even at environmentally relevant concentrations [11].

In the EU, dimoxystrobin was first authorized in 2006, and its approval period ultimately lasted for 17 years. In 2023, based on the evidence reported by the EFSA [12], the European Commission did not renew the authorization of dimoxystrobin due to several concerns, including the lack of accurate data assessing the risk for honeybee larvae, and the high acute risk to aquatic invertebrates. Due to its chemical properties, such as long aqueous photolysis and hydrolysis time, dimoxystrobin is persistent in both soil (degradation value ranging from 423.1 to more than 1000 days) and water systems [13,14]. Moreover, the pesticide risk assessment released by EFSA clearly refers to the potential for groundwater contamination by the metabolites of dimoxystrobin [12]. A recent study on the southern China rivers revealed the presence of dimoxystrobin in 78.4% of analyzed surface water samples [11].

Dimoxystrobin has been classified as moderately toxic to birds and highly toxic to earthworms based on acute toxicity tests. Despite this, dimoxystrobin continues to be commercialized in several countries, including the United Kingdom and Brazil. Limited data is available regarding dimoxystrobin's impact on aquatic biota, with most studies focusing on short-term toxicity to some fish and invertebrate species [15]. Particularly in fish, the sublethal effects of dimoxystrobin remain largely under investigated, creating a knowledge gap that needs to be filled to fully understand its harmful potential. Yet, recent evidence supports the toxicity of dimoxystrobin in fish, and we demonstrated that this fungicide induces severe structural and ultrastructural alterations in the gills of adult *Danio rerio*, even at environmentally relevant concentrations [16]. Moreover, it impairs embryos' development and swimming performance in the same species and modulates genes related to the mitochondrial respiratory chain [17].

In fish, the liver plays a fundamental role in the metabolism of proteins, lipids, and carbohydrates, as well as in the process of biotransformation, detoxification of xenobiotics, and excretion [18,19]. The liver has been identified as a sensitive target of environmental pollutants, and the alterations occurring in this organ can be used to predict the impacts at organism level [20,21]. Surprisingly, in fish, only one report investigated metabolic disorders and the antioxidant enzyme modulation following chronic exposure to high dimoxystrobin concentrations [22].

Danio rerio has been elected by different organizations as a useful experimental model for studying organ changes after chemical exposure (the Organization for Economic Cooperation and Development—OECD and the International Organization for Standardization—ISO). Furthermore, the zebrafish genome has notable homology with that of the human genome, and 70% of human genes have zebrafish orthologues, justifying its growing use in translational research [23–25].

Starting from this background, we investigated for the first time the effects of dimoxystrobin on zebrafish liver after short-term exposure (96 h) to two sublethal and environmentally relevant concentrations (6.56 and 13.13 µg/L) [11,26]. Histopathological studies allow the early detection of pollutant-induced damage, often before any visible signs or clinical symptoms emerge [27]. Therefore, we first evaluated the liver histology and conducted an objective assessment of the structural damage using a semi-quantitative method [28,29]. Since the liver plays a crucial role in glucose metabolism and lipid homeostasis [30], we also quantified the amounts of storage products (i.e., glycogen granules and lipid droplets) through a morphometric approach [31]. The ultrastructural approach is not frequently used in ecotoxicological studies, although morphological alterations at the subcellular level can provide important indications of potentially compromised cellular function [31–33]. In this study, we assessed both histological and subcellular changes to provide a comprehensive overview of dimoxystrobin-induced morphological effects.

Considering the mode of action of strobilurins, involving an increased generation of reactive oxygen species (ROS) [34,35], we then evaluated the expression of superoxide dismutase (SOD) and catalase (CAT), two well-recognized markers of oxidative stress [36]. The results presented here provide further insights into the adverse effects of dimoxystrobin in fish and aim to contribute to the debate on the risks posed by strobilurins to aquatic species. Our study highlights the role of a joint morphological and functional analysis in assessing the effects of pollutants at sublethal doses.

2. Materials and Methods

2.1. Fish Maintenance

Adult zebrafish (AB wild-type; 6–8 months old) of both sexes were housed in the zebrafish facility (Department of Biological Science at the University of Bergen) according to the European Convention for the Protection of Vertebrate Animals Used for Experimental and Other Scientific Purposes. Animals were maintained in a recirculating system at 26–28 °C, under a 14/10 light–dark photoperiod and were fed twice daily with *Artemia salina*.

2.2. Test Substance

To obtain the two selected concentrations of dimoxystrobin, a stock solution of 1000 µg/L dimoxystrobin (purity ≥ 98.0%, Sigma-Aldrich Chemical Co., Gillingham, UK) was first prepared by dissolving 1000 µg of the fungicide in 100 µL of acetone and then diluting it in 1000 mL of water from the zebrafish facility system. The stock solution (1 mg/L) was further diluted (in facility systems water) to obtain the selected concentrations of dimoxystrobin (6.56 and 13.13 µg/L, low and high concentrations, respectively). The low and high doses correspond to the 40% and 80% of dimoxystrobin's predicted environmental concentration in freshwater (PEC_{fw} = 16.42 µg/L), respectively [33]. In the control group, the same amount of the solvent was added (less than 0.001% v/v). A preliminary test confirmed that acetone did not induce a discernable effect on zebrafish adults at similar concentrations, as reported by other authors [37,38].

The chemical analysis of dimoxystrobin in water samples was performed as previously described by Ahmed and colleagues [16]. The measured concentrations of dimoxystrobin samples were 6.58 ± 0.10 and 13.66 ± 0.33 µg/L for the low and high concentrations, respectively.

2.3. Experimental Design

G*Power 3.1.9.7 software (Franz Faul, Universität Kiel, Germany) was employed, following the 'a priori' method, to determine the minimum number of animals required for this study. Animals (n = 42) were randomly assigned to the different experimental units: control, 6.56 µg/L (referred to as the low concentration group) and 13.13 µg/L (referred to as the high concentration group). Fourteen fish were placed in 30 L tanks (40 × 32 × 20 cm, n = 3) containing the appropriate solution for each group.

Animals were exposed to a static system with the test solutions renewed daily following the OECD Guidelines [39,40] with slight modifications. All experiments were approved by the Norwegian Food Safety Authority (Permit number FOTS ID 29916). Throughout the duration of the experiment (96 h), the fish were not fed and all parameters were monitored and kept constant. Three independent biological replications of the entire experiment were performed. No mortality was registered throughout the exposure period.

After 96 h of exposure, the fish were euthanized. They were first immersed in buffered MS222 (0.20 mg/mL; approximately for 10–30 s) and then put for 10 min in an ice-chilled water bath (0–4 °C) to induce hypothermic shock [41]. After removal, liver samples were then processed according to the standard protocol for morphological and molecular analyses.

2.4. Histological and Ultrastructural Methods

For each experimental group, including the control, seven animals were used to perform morphological and ultrastructural analyses. Liver samples were fixed in 3% glutaraldehyde (Electron Microscopy Sciences, Hatfield, PA, USA) in 0.1 M phosphate-buffered saline solution (PBS, pH 7.2) for 3 h. Samples post-fixed for 2 h at 4 °C in 2% osmium tetroxide (Electron Microscopy Sciences, Hatfield, PA, USA) were then dehydrated with increasing ethanol concentrations. Finally, the samples were immersed in propylene oxide and embedded in Epon-Araldite (Araldite 502/Embed 812, Electron Microscopy Sciences, Hatfield, PA, USA). Semi-thin sections (1 µm) and ultra-thin sections (800 Å) were obtained using a Leica UltraCut UCT (Leica Microsystems, Wetzlar, Germany). Semi-thin sections were stained with toluidine blue (1% toluidine in 2% borate) and observed under a light microscope (DM1000 LED; Leica Microsystems, Wetzlar, Germany) equipped with an Optika HDMI Digital Camera. Ultra-thin sections were stained with uranyl acetate, contrasted with lead citrate (Electron Microscopy Sciences, Hatfield, PA, USA), and examined under a JEM 1400 PLUS electron microscope (JEOL, Peabody, MA, USA).

2.5. Histopathological and Morphometrical Analyses

The histopathological investigations were conducted using a semi-quantitative approach [28,42] that enables the determination of the severity of histological changes. For each animal (n = 7) of each treated group, including the control, all the detected alterations were classified into four distinct reaction patterns (circulatory, regressive, progressive, and inflammation changes). Then, an importance factor ranging from 1 (minimum pathological importance) to 3 (marked pathological importance) was given based on the relevance of the change and its pathological value. Finally, score values were assigned based on the degree and extent of each detected pathological change: 0 = unchanged, 2 = mild occurrence, 4 = moderate occurrence, and 6 = severe occurrence (Table S1). To ensure standardization of the histopathological analysis, all score values were assigned by the same operator.

The organ index (I_{org}), which allows the extent of organ damage to be determined, was finally calculated using the importance factor and the score value employing the formula reported below:

$$I_{org} = \Sigma_{rp}\, \Sigma_{alt}(a_{\ rp\ alt} \times w_{\ rp\ alt})$$

where rp = reaction pattern; alt = alteration; a = score value; and w = importance factor.

2.6. Lipid Droplet and Glycogen Granule Content

Lipid droplet and glycogen granule content was evaluated on semi-thin sections (stained with toluidine blue) following the method described by Macirella et al. [42,43]. For each animal in the control and dimoxystrobin-treated groups (n = 7), five non-consecutive liver sections were observed and photographed at a magnification of 100×. To make an objective measurement, we used a specific selection tool from the free and open-source ImageJ 1.53k software (NIH, developed by the National Institutes of Health, a part of the U.S. Department of Health and Human Services) to define the boundary of the lipid droplets or the glycogen granules in each micrograph. Lipid droplets or glycogen granules were isolated, and the total area was measured and expressed as the percentage of area occupied by the lipid droplet or the glycogen granules in each section. Data were finally statistically compared to determine significant differences among groups.

2.7. RNA Isolation and qRT-PCR

Total RNA was extracted from seven treated and non-treated animals using the PureLink RNA Mini Kit and PureLink™ DNase Set (Thermo Fisher Scientific, Waltham, MA, USA), following the manufacturer's recommendations. The quantity and quality of the total RNA extract were determined by A_{260nm}/A_{280nm} ratio (absorbance ratios > 1.8) using a NanoDrop One device (Thermo Fisher Scientific, Waltham, MA, USA) and 1.5% agarose gel electrophoresis, respectively.

Purified RNA was used for first-strand cDNA synthesis and reverse transcribed using the high-capacity RNA to cDNA kit (Applied Biosystems, Foster City, CA, USA) according to the manufacturer's instructions. The obtained cDNA was kept at −20 °C until qRT-PCR analysis, which was performed using the TaqMan Gene Expression Assay (Thermo Fisher Scientific, Waltham, MA, USA) in a Light Cycler (Applied Biosystems StepOne, Real-Time PCR System, Foster City, CA, USA). The following amplification cycles were used: one cycle at 50 °C for 2 min, one cycle at 95 °C for 10 min, 40 cycles at 95 °C for 15 s, and one cycle at 60 °C for 60 s. The qRT-PCR reactions, with a final volume of 20 µL, contained 10 µL of master mix (TaqMan Universal Master Mix II, Applied Biosystems), 1 µL of assay mix (TaqMan Gene Expression Assay), 7 µL of RNase/DNase-free H2O, and 2 µL of cDNA. The target genes were superoxide dismutase 1 (*sod1*, NCBI Reference Sequence: NM_131294.1) and catalase (*cat*, NCBI Reference Sequence: NM_130912.2). For both genes, three technical replicates were performed. The relative mRNA expression was normalized according to the average expression level of the actin beta 1 (*actb1*, NCBI Reference Sequence: NM_131031.2) and the glyceraldehyde-3-phosphate dehydrogenase (*gapdh*, NCBI Reference Sequence: NM_001115114.1) and calculated with the $2^{-\Delta\Delta CT}$ comparative CT method [44].

2.8. Statistical Analyses

All statistical analyses were performed at a 0.05 significance level using the GraphPad Prism 8.00 software (GraphPad Software Inc., San Diego, CA, USA). The results of the different biological replicates were compared using the Mann–Whitney test. The replicates did not show significant differences ($p > 0.05$); hence, the data were combined for further analysis. The one-way ANOVA followed by Dunn's multiple comparison test was employed to statistically compare significant differences in the organ index between the dimoxystrobin-treated and control groups. The one-way ANOVA followed by Tukey's multiple comparison test was used to statistically compare morphometrical parameters and mRNA expression levels among dimoxystrobin-treated and control groups. The assumption of normality was tested with the Kruskal–Wallis (organ index) or the Shapiro–Wilk tests (morphometrical parameters and gene expression). For all tests, the homoscedasticity was verified using the Brown–Forsythe test.

3. Results

3.1. Histology and Ultrastructure

3.1.1. Control Group

The histology and ultrastructure of *Danio rerio* liver are similar to those of other freshwater teleosts and have been previously described [18,42,43]. Here, a concise outline relevant to the present analysis will be provided. Light microscopy (LM) observations revealed compact and uniform liver parenchyma composed of hepatocytes, which formed a cord-like structure surrounding a network of sinusoids (Figure 1a,b). The sinusoid lumen is lined by thin, flattened endothelial cells with protruding nuclei (Figure 1b). It is possible to identify the perisinusoidal space (i.e., space of Disse) between the endothelial and parenchymal cells (Figure 1b). The veins of various sizes and shapes and minute bile channels were scattered among the hepatocytes (Figure 1a,b). In the lumen of veins and sinusoids, some nucleated erythrocytes and a few macrophages were visible (Figure 1b). Polygonal hepatocytes typically have a large, rounded nucleus centrally located, along with a prominent nucleolus (Figure 1b). Scattered throughout their cytoplasm, lipid droplets and numerous glycogen granules were observed (Figure 1b).

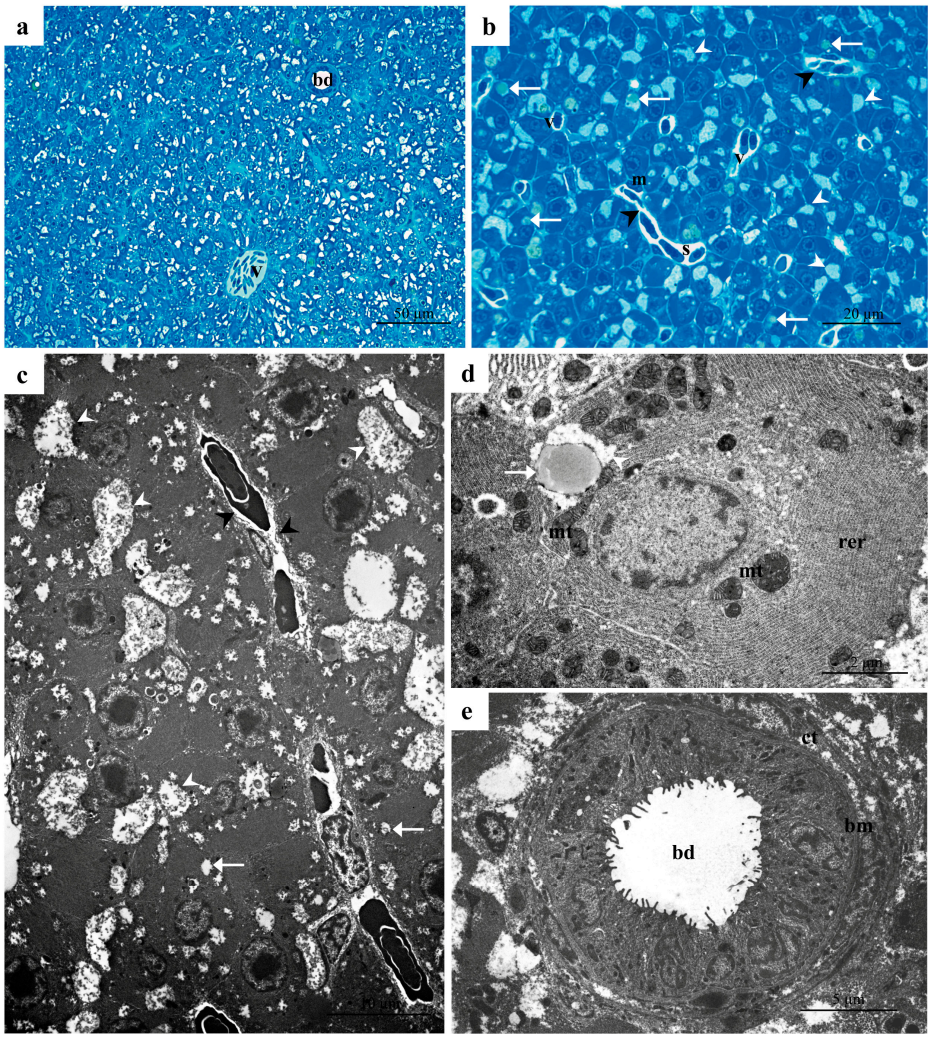

Figure 1. Representative micrographs of *Danio rerio* liver under basal conditions. (**a**,**b**) Light micrographs showing sinusoids (s), veins (v) and bile ducts (bd) scattered in the parenchyma. Note the space of Disse that lies between the hepatocytes and the sinusoidal endothelium (black arrowheads). White arrows = lipid droplets; white arrowheads = glycogen granules; m = macrophages. (**c**,**d**) TEM micrographs showing numerous mitochondria (mt), the prominent endoplasmic reticulum (rer), the glycogen granules (white arrowheads) and a few lipid droplets (white arrow) in the cytoplasm of hepatocytes; black arrowheads = space of Disse. (**e**) Detail of bile duct (bd) enclosed by cuboidal epithelium; note the basal membrane (bm) and the thin layer of connective tissue (ct).

Under TEM, the hepatocytes showed a spherical nucleus characterized by a low amount of heterochromatin and a wide nucleolus. Their cytoplasmic matrix was electron-dense (Figure 1c,d), with a prominent rough endoplasmic reticulum (RER) extending from the perinuclear area toward the cell periphery (Figure 1c,d). Numerous mitochondria with high electron density were scattered through the cytoplasm, often associated with RER cisternae (Figure 1c,d). The rosette-shaped glycogen granules and a few lipid droplets were mainly located in the hepatocyte's peripherical area (Figure 1d).

The bile ducts are rounded channels lined by a simple cuboidal epithelium surrounded by the basal membrane and a thin layer of connective tissue (Figure 1e). Cubic cells, with a high nuclear-cytoplasmic ratio, are joined to each other and bear numerous microvilli projecting on the luminal surface (Figure 1e).

3.1.2. Low-Concentration Group (6.56 µg/L)

The histological examination of the liver after exposure to the low dimoxystrobin concentration revealed several pathological changes. The appearance of lysed areas is one of the many signs of cell degeneration, which compromises the arrangement of liver parenchyma (Figure 2a–c).

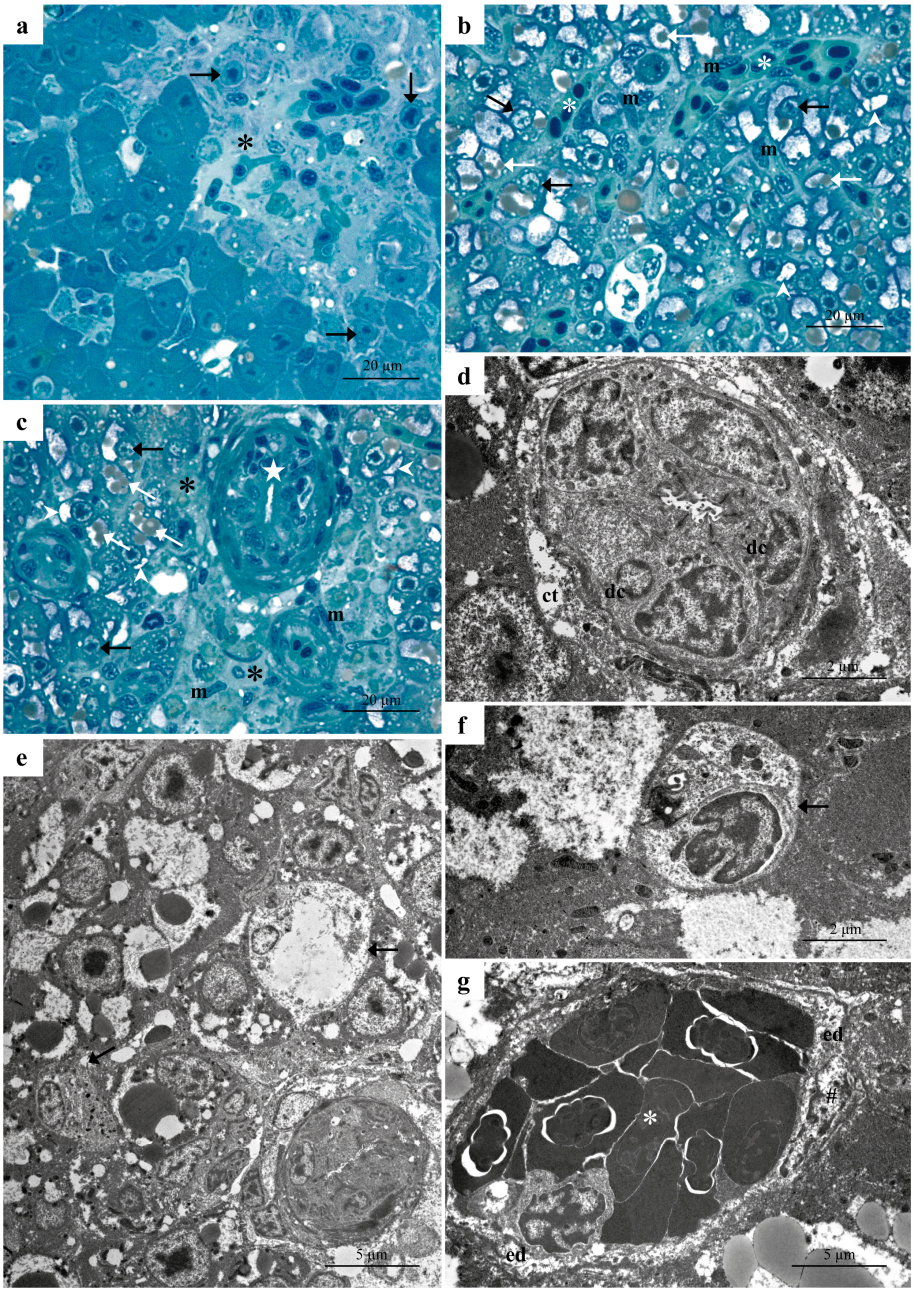

Figure 2. Representative micrographs of *D. rerio* liver after exposure to the low concentration of dimoxystrobin. (**a**–**c**) Light micrographs showing lysed areas (black asterisks) and the congestion of blood vessels and sinusoids in the liver parenchyma (white asterisks). Note the proliferation of macrophages (m) and numerous necrotic hepatocytes (black arrows). White arrowheads = glycogen granules; white arrows = lipid droplets; white stars = bile duct obstruction. (**d**) TEM micrograph showing lacunae in the connective tissue surrounding the bile ducts (ct) and the degeneration of cuboidal cells (dc). (**e**,**f**) Necrotic cells are characterized by poor, pale-stained cytoplasm and the disorganization of cellular organelles (black arrows). (**g**) Detail of vessel congestion (white asterisk); note the detachment of the endothelium (ed) and the degeneration of the endothelial cell (hashtag).

In these areas, degenerating necrotic cells are associated with inflammatory loci (Figure 2a). Numerous hepatocytes displayed a vacuolized cytoplasm, thus indicating a progression to a necrotic phenotype (Figure 2b,c). A decrease in rosette-shaped glycogen granules was also observed, along with an increase in lipid droplet amount (Figure 2b,c). Macrophages were often detected in the veins and sinusoids and they also proliferated in the liver parenchyma (Figure 2b,c). The obstruction of the bile ducts was noted where cuboidal cell swelling occurs (Figure 2c). Numerous blood vessels and sinusoids were congested (Figure 2b)

Ultrastructural observation allowed us to appreciate better the degenerative changes affecting the cuboidal cells as well as the formation of large lacunae in the connective tissues surrounding the biliary ducts (Figure 2d). Severe ultrastructural changes occurred in the hepatocytes that often showed necrotic features (Figure 2e,f). It was possible to note the poor, pale-stained cytoplasm and the complete disorganization of cellular organelles of necrotic hepatocytes (Figure 2e) better appreciable with further enlargement (Figure 3f). Numerous erythrocytes and macrophages had accumulated in the lumen of blood vessels, which appeared congested (Figure 2g). An extensive detachment of the endothelium was also noted and, in some cases, it was possible to observe the degeneration of the endothelial cells (Figure 2g).

3.1.3. High-Concentration Group (13.13 μg/L)

Histological analysis of the liver revealed extensive pathological modification following exposure to the high concentration of dimoxystrobin. The structural and ultrastructural alterations described in samples from the low-concentration group were detected with high frequency and severity. The presence of extensively lysed areas disrupted the usual arrangement of liver parenchyma. (Figure 3a). Proliferating macrophages were observed in the lumens of vessels and sinusoids, as well as scattered throughout the liver parenchyma (Figure 3a,b). The accumulation of numerous blood cells and macrophages in the lumen of vessels and sinusoids led to their congestion (Figure 3c). ccumulation of numerous lipid granules and cytoplasm vacuolization were often observed in hepatocytes, while the content of glycogen granules was dramatically reduced (Figure 3b,c). Numerous necrotic hepatocytes with pale cytoplasm were often seen (Figure 3b,c). The bile duct's arrangement is markedly modified, showing a reduced lumen and an evident degeneration of cuboidal cells (Figure 3b).

Observations conducted under TEM allowed us to better appreciate the disorganization of the liver parenchyma and degenerative features of hepatocytes (Figure 3d–h). With further enlargement, it was possible to detect ultrastructural features of necrotic cells. In their poor and lightly stained cytoplasm, fragmented rough endoplasmic reticulum was seen, confined at the periphery of the cells, while degenerating mitochondria were still recognizable (Figure 3d,e). At several points, the nuclei of hepatocytes appeared severely damaged, showing a change in the distribution and amount of heterochromatin (Figure 3d). Apoptotic cells were characterized by an electron-dense cytoplasm in which a conspicuous nucleus and apoptotic bodies could be detected (Figure 3f). Numerous melanomacrophage centers could also be detected scattered through the parenchyma (Figure 3g). These nodular clusters of macrophages often showed a cytoplasm rich in heterogeneous electron-dense granules (Figure 3g). The degeneration of the bile ducts was extensive and severe; the typical arrangement of the biliary cells was completely lost, and they assumed a disorganized appearance (Figure 3h). In some cases, some cuboidal cells were degenerated and also showed pyknotic nuclei (Figure 3h).

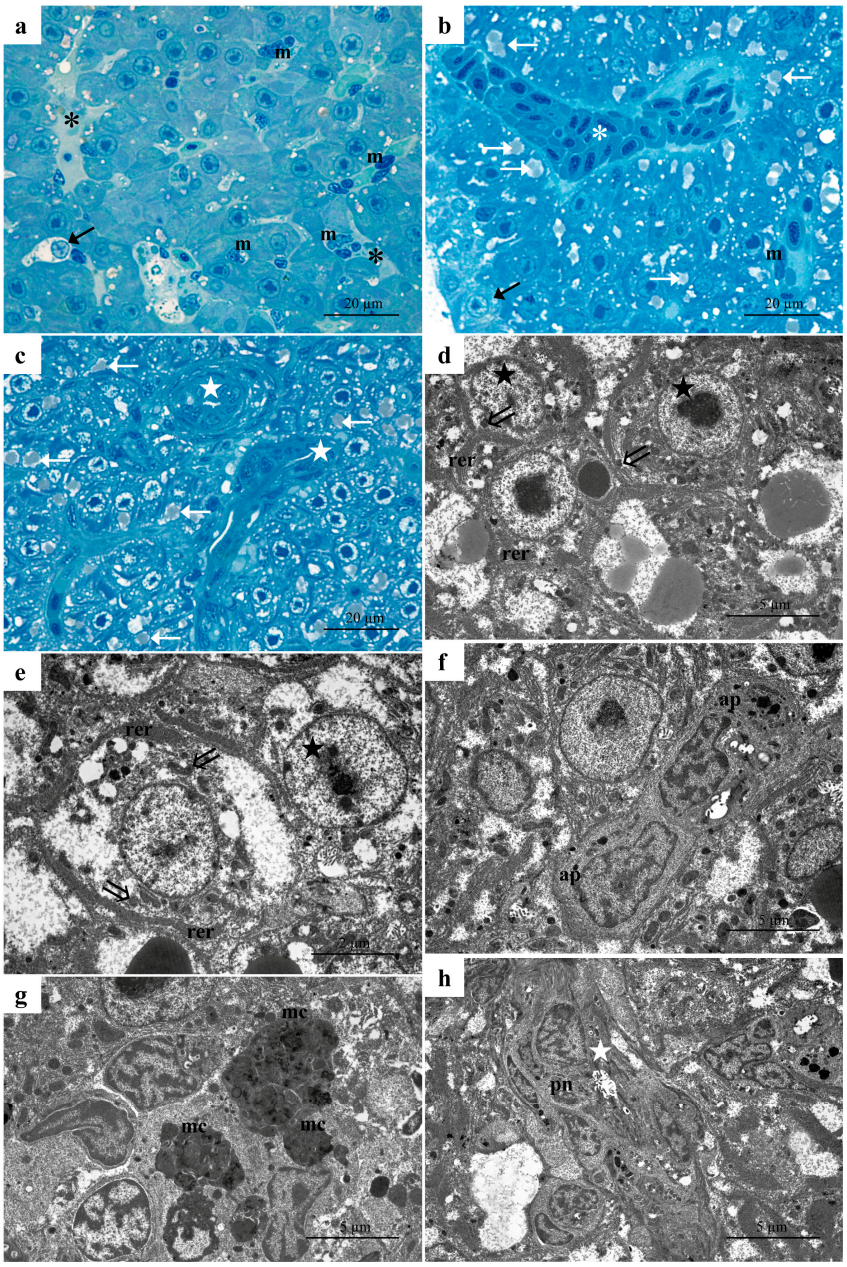

Figure 3. Representative micrographs of *D. rerio* liver after exposure to the high concentration of dimoxystrobin. (**a**–**c**) Light micrographs showing extensively lysed areas (black asterisks) and the proliferation of macrophages in both vessels and liver tissue (m). Note the degeneration of bile ducts (white stars) and the congestion of blood vessels (white asterisk). White arrows = lipid droplets. (**d**,**e**) TEM micrographs of necrotic cells showing fragmented rough endoplasmic reticulum (rer) and degenerating mitochondria (double arrows) and nuclei (black stars). (**f**) Detail of apoptotic cells (ap). (**g**) Melanomacrophage centers are characterized by a cytoplasm rich in heterogeneous electron-dense granules (mc). (**h**) Note the degeneration of the bile duct (white star) and the pyknotic nuclei of cuboidal cells (pn).

3.2. Organ Index

The statistical analysis of the organ index, representing the extent of organ damage, revealed a significant correlation between tissue injury and dimoxystrobin concentration (Table 1). Exposure to the low dimoxystrobin concentration significantly increased the organ index compared to the control. When the high concentration was administered, a

further increase in the organ index was observed, which was significantly higher compared to both the control and low-concentration groups.

Table 1. Organ index.

CTRL	6.56 µg/L DMX	13.13 µg/L DMX
3.50 ± 1.91	31.00 ± 5.03 $^{(a****)}$	47.00 ± 1.15 $^{(ab****)}$

Class I (index ≤ 10) normal organ structure; Class II (index 11–20) slight histological alterations; Class III (index 21–30) moderate histological alterations; Class IV (index 31–40) pronounced histological alterations of the organ; Class V (index > 40) severe histological alterations. a = significant differences between the treatment and control groups ($p \leq 0.0001$). b = significant differences between the high- and low- concentration groups (**** $p \leq 0.0001$).

3.3. Morphometric Analyses

Morphometric analysis revealed that the glycogen content and lipid droplet underwent substantial modification following dimoxystrobin exposure.

Lipid droplet content—A significant increase was seen in both treatment groups compared to the control (Figure 4a). Specifically, samples exposed to the low concentration exhibited a significant increase compared to the control. In contrast, the increase detected in the high-concentration group was statistically significant compared to the control and low-concentration groups (Figure 4a).

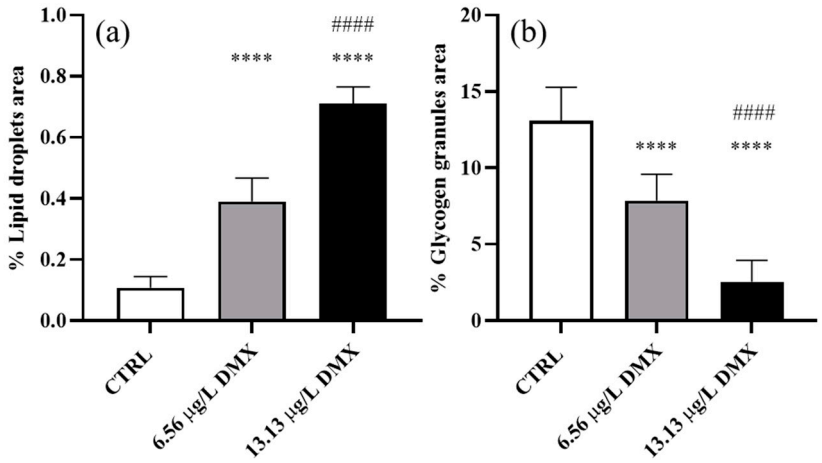

Figure 4. The percentage of area occupied by lipid droplets (**a**) and glycogen granules (**b**) in *Danio rerio* liver after exposure to dimoxystrobin. Data are represented as mean ± SD. Asterisks indicate significant differences between the treatment and control groups. Hashtags show significant differences between the high- and low-concentration groups. **** $p \leq 0.0001$; #### $p \leq 0.0001$.

Glycogen granule content—A significant decrease in glycogen granule content was seen in the exposed groups compared to the control, and the decrease followed a dose-dependent trend. The glycogen amounts significantly decreased in the low-concentration group compared to the control, reaching the lowest value in the high-concentration group when a significant difference could also be detected compared to the low and high-exposure groups (Figure 4b).

3.4. Real-Time PCR (qRT-PCR)

Sod and *cat* gene expression showed a significant decrease after exposure to low and high concentrations of dimoxystrobin (Figure 5a,b). In particular, exposure to the low concentration induced a significant downregulation compared to the control group. The expression slightly increased after exposure to the high concentration, although it remained significantly lower than in the control group.

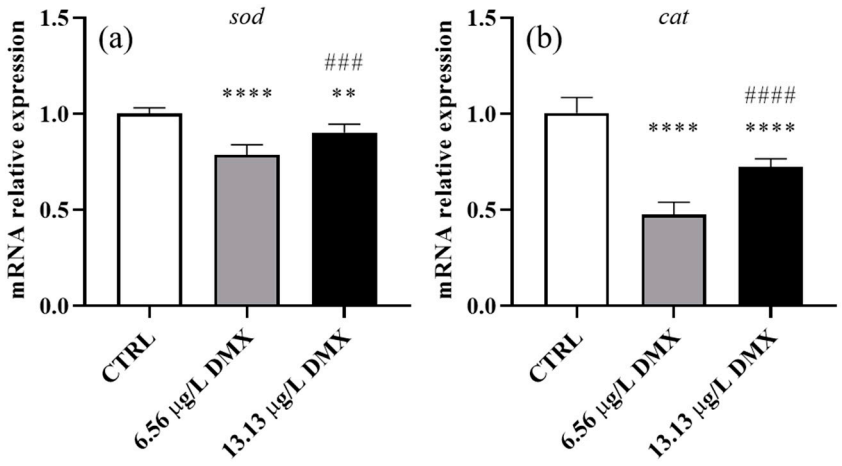

Figure 5. Relative gene expression of superoxide dismutase (**a**) and catalase (**b**) in *Danio rerio* liver after exposure to dimoxystrobin. Data are represented as mean ± SD. Asterisks indicate significant differences between the treatment and control groups. Hashtags indicate significant differences between the high- and low-concentration groups. ** $p \leq 0.01$; **** $p \leq 0.0001$; ### $p \leq 0.001$; #### $p \leq 0.0001$.

4. Discussion

Irrespective of the intake route (e.g., gills, skin, and digestive tract), the liver of fish and other vertebrates is called upon to fulfil its role in detoxification and excretion, thus representing an obvious target for xenobiotic substances, including fungicides [42]. When the liver undergoes morphological or functional modifications, its crucial role in maintaining metabolic activities and homeostasis is compromised, interfering with the overall physiological functioning of the organism [45]. In fish, hepatotoxic effects are recognized as indicators of biological status and are widely used as biomarkers in environmental risk assessments [46]. In the present study, we investigated the sublethal effects induced by dimoxystrobin on *Danio rerio* liver for the first time, providing evidence of morphological, functional, and ultrastructural modifications. The doses tested in our experiments were very low and environmentally relevant, thus unveiling the high toxicity of this fungicide in fish.

4.1. Morphology and Ultrastructure

Exposure to dimoxystrobin induces several pathological responses in *Danio rerio* liver that can be attributed to four reaction patterns (circulatory disturbances, regressive changes, progressive changes, and inflammation). Both the degree and severity of these harmful effects increased in a concentration-dependent manner.

Circulatory disturbances, such as blood vessels and sinusoid congestion, were among the most frequently detected alterations in both exposed groups. Similar changes have been previously reported in the same species after exposure to strobilurins and azole fungicides [43,47]. These alterations are considered reversible since they are supposed to regress once the toxicant input is removed, and they do not alter the normal functioning of the tissue [42,48].

Regressive changes that include cell degeneration and the consequent appearance of the lysed area were frequently detected in the liver of both exposed groups, with a higher incidence in the group exposed to the high concentration. The onset of the degenerative phenomena of both apoptotic and necrotic types is one of the outcomes of exposure to strobilurins and other fungicides in freshwater fish [43,47,49,50] supporting the hypothesis that such pesticides share the ability to induce tissue injury through both mechanisms. Ultrastructural observation allowed us to discriminate between apoptosis and necrosis reliably, thus revealing that the liver cells mainly underwent necrotic degeneration in both exposed groups. Still, the apoptotic phenotype occurred more frequently in samples

exposed to the high concentration. It must be pointed out that necrotic events are considered a direct effect of toxic input and are generally classified as irreversible alterations of the tissue that ultimately impair organ function [48].

In our study, we frequently observed numerous macrophages in vessels and sinusoid lumen that proliferated to the liver parenchyma. There is substantial documentation showing that hepatic macrophages are involved in liver disease progression in vertebrates. When liver damage occurs, resident macrophages infiltrate the tissue to remove aged and altered hepatocytes and maintain tissue homeostasis [51]. In fish, the data on the presence and role of macrophages are not exhaustive, leaving several questions about their origin and functions [52]. Among the most common pathological effects in the liver of fish exposed to pollutants is the presence of melanomacrophage aggregates, also called melanomacrophage centers (MMCs), a distinctive group of pigment-containing cells usually found in the spleen, liver and kidney of fish [53]. Melanomacrophage infiltration has been documented under pathological conditions due to its putative role in immunity, and it is particularly common in conditions characterized by inflammation [52,54]. Moreover, MMCs are involved in the phagocytosis of cellular debris [55], and it has been suggested that their increase could be related to both inflammatory responses and the detoxification of exogenous and endogenous substances [19]. Furthermore, their melanin content indicates a role in the antioxidant response due to the compound's ability to sequester redox-active metal ions and scavenge oxidizing free radicals [52] and references therein.

In our study, macrophage aggregates (i.e., melanomacrophage centers) were detected in the liver samples from both exposed groups, being more conspicuous in the high-concentration group, thus suggesting that the increase in MMCs would be one of the main reaction patterns through which the fish liver responds to the dimoxystrobin insult.

4.2. Morphometric Evaluation

In fish, exposure to pollutants may interfere with the energetic storage of the organism, inducing a decrease in the glycogen amount, which represents the most common response to pesticide exposure [18,19,56,57]. Compared to other organs, glycogen depletion is greater in the liver since it is the primary site of its synthesis and storage [19,58]. In the present study, we observed a significant dose-related reduction in glycogen granules in zebrafish hepatocytes following exposure to dimoxystrobin.

The literature provides several evidence for hepatic glycogen depletion in freshwater fish after exposure to fungicides [43,59,60] and other pesticides [61–63].

It seems that decreased glycogen content is a pathological pattern shared by strobilurins and other pesticides. This is not surprising as, according to the literature data, under stress conditions, the glycogen reserves deplete to meet energy demand [56,63,64], regardless of the specific types of induced insult. It is worth noting that in the present study the depletion of glycogen content was observed after just 96 h of exposure, suggesting that it may increase over the long term, potentially leading to unavoidable consequences on the overall health of the exposed animals.

Lipid accumulation in the liver is a commonly detected outcome of xenobiotic exposure [42,43,65,66]. In the liver, an increase in lipid droplets has been documented in different freshwater fish after exposure to several pesticides, including fungicides [43,65,66]. In the present study, a significant increase in lipid granules was a pathological reaction found in the samples exposed to dimoxystrobin, also showing a dose-dependent trend. In the liver of bighead carp (*Hypophthalmichthys nobilis*), a similar increase in lipid inclusion was observed after exposure to two pesticides; notably, accumulation increased with the rise in the tested dose.

It has been suggested that the hepatic accumulation of lipid droplets would be related to lipid metabolism dysfunction [67] or the impossibility of exporting them from the cells [68]. Several authors also suggested that increased lipid accumulation may be indicative of an inflammatory process in response to oxidative stress. Our morpholog-

ical and ultrastructural examinations revealed a substantial inflammatory response to dimoxystrobin in liver tissue, thereby supporting this hypothesis.

4.3. Oxidative Stress

The mitochondrial cytochrome *bc1* complex has been identified as the primary source of reactive oxygen species (ROS) in the mitochondrial respiratory chain [69,70]. ROS generation might lead to the inhibition or overproduction of enzymes involved in antioxidative defense systems, including superoxide dismutase (SOD) and catalase (CAT) [71,72]. In the liver of *Danio rerio* and other freshwater species, both the increased and decreased activity of such enzymes have been documented after exposure to strobilurins [73–78]. Here we showed a significant downregulation of *sod* and *cat* in the liver after exposure to both dimoxystrobin concentrations. A similar decrease was previously reported in common carp (*Cyprinus carpio*) liver after 15 days of exposure to the minimal lethal dose of dimoxystrobin [22], and this pattern is not new for strobilurins. Superoxide dismutase (SOD) and catalase (CAT) levels were remarkably reduced in the hepatopancreas of *Danio rerio* and *Cyprinus carpio* exposed to pyraclostrobin [78,79]. Decreased CAT activity was reported in zebrafish embryos exposed to pyraclostrobin and trifloxystrobin [8]. Additionally, reduced SOD activity was observed in juvenile grass carp (*Ctenopharyngodon idella*) exposed to three strobilurins (pyraclostrobin, trifloxystrobin and kresoxim-methyl) [80]. Several hypotheses have been proposed to explain the depletion of the antioxidant enzyme activity induced by strobilurins and other pollutants, including a direct effect of toxic compounds on the chemical structure of such enzymes [81] and an inhibition due to the ROS accumulation in the tissues [78].

It must be pointed out that the tissue-specific response of SOD and CAT to pesticide exposure is not a novel item, and it has been reported in several freshwater fish exposed to pesticides, including strobilurins [82–84]. As previously suggested, to neutralize oxidative stress, different adaptive responses may be mounted in different tissues [82,83,85]. Furthermore, fundamental differences in the blood volume reaching different organs may lead to a different interstitial concentration of xenobiotics, explaining the differences observed in antioxidant response [82,86].

We recently showed a significant increase in *sod* and *cat* expression in the gills of *Danio rerio* after exposure to dimoxystrobin under the same experimental conditions described here [16], thus supporting the hypothesis that the antioxidant response to strobilurins is both species- and tissue-specific [83].

4.4. Limitations of the Study

It is important to note a critical limitation of our study. This study aimed to evaluate the sublethal effects of dimoxystrobin on zebrafish liver. Still, the aim of the research was not to compare the effects induced by increasing concentrations of such fungicide, which would require testing at least one other intermediate concentration. We chose to test only two doses in order to limit the number of animals used in the study.

5. Conclusions

The present study demonstrated for the first time that two environmentally relevant concentrations of dimoxystrobin considerably affect zebrafish liver even after short-term exposure, inducing both histological and ultrastructural modifications. Some of these alterations can be considered reversible (i.e., circulatory disorders), while others are regressive and include necrotic and apoptotic events. The increase in macrophage aggregates in the liver samples from both exposed groups suggests that this may be one of the main reaction patterns through which the fish liver responds to the dimoxystrobin insult. Our morphometrical analysis also revealed a significant increase in lipid content and a decrease in glycogen granules, thus highlighting the potential of this fungicide to induce metabolic dysfunctions. In addition, this fungicide impairs the expression of key enzymes involved in the defensive response against oxidative stress. Overall, our research emphasizes the

importance of integrating multiple end-points when assessing the toxic effects of pesticides. In our opinion, this approach ensures the collection of detailed information on subtle sublethal effects, which is essential for the toxicity assessment of currently used and new agrochemical compounds.

Supplementary Materials: The following supporting information can be downloaded at: https://www.mdpi.com/article/10.3390/environments11120282/s1, Table S1: Histopathological evaluation tool.

Author Contributions: Conceptualization, E.B.; methodology, M.M. and N.G.; software, M.M. and A.I.M.A.; formal analysis, R.M. and F.T.; investigation, A.I.M.A., R.M. and F.T.; writing—original draft preparation, A.I.M.A., R.M. and E.B.; writing—review and editing, E.B.; supervision, E.B.; project administration, E.B. All authors have read and agreed to the published version of the manuscript.

Funding: This research received no external funding.

Data Availability Statement: The original contributions presented in this study are included in the article/Supplementary Materials. Further inquiries can be directed to the corresponding author(s).

Conflicts of Interest: The authors declare no conflicts of interest.

References

1. Herrero, M.; Thornton, P.K.; Power, B.; Bogard, J.R.; Remans, R.; Fritz, S.; Gerber, J.S.; Nelson, G.; See, L.; Waha, K.; et al. Farming and the geography of nutrient production for human use: A transdisciplinary analysis. *Lancet Planet. Health.* **2017**, *1*, e33–e42. [CrossRef]
2. Bindraban, P.S.; Dimkpa, C.O.; Angle, S.; Rabbinge, R. Unlocking the multiple public good services from balanced fertilizers. *Food Secur.* **2018**, *10*, 273–285. [CrossRef]
3. Macirella, R.; Madeo, G.; Sesti, S.; Tripepi, M.; Bernabò, I.; Godbert, N.; La Russa, D.; Brunelli, E. Exposure and post-exposure effects of chlorpyrifos on Carassius auratus gills: An ultrastructural and morphofunctional investigation. *Chemosphere* **2020**, *251*, 126434. [CrossRef] [PubMed]
4. Nagesh, P.; Edelenbosch, O.Y.; Dekker, S.C.; de Boer, H.J.; Mitter, H.; van Vuuren, D.P. Extending shared socio-economic pathways for pesticide use in Europe: Pest-Agri-SSPs. *J. Environ. Manag.* **2023**, *342*, 118078. [CrossRef] [PubMed]
5. EUROSTAT. Agri-Environmental Indicator-Consumption of Pesticides. 2024. Available online: https://ec.europa.eu/eurostat/statistics-explained/index.php?title=Agri-environmental_indicaPandeytor_-_consumption_of_pesticides (accessed on 16 September 2024).
6. Pandey, G.; Rathore, H. Toxicity of Strobilurins fungicides: A comprehensive review. *J. Chem. Health Risks* **2023**, *13*, 207–218. [CrossRef]
7. Weaver, C.R.; Brockman, M.; Mundahl, N.D.; Arnold, W.A.; Blumentritt, D.; Varela, W.L.; Franz, J.L. Detection of strobilurin fungicides in trout streams within an agricultural watershed. *Hydrology* **2024**, *11*, 13. [CrossRef]
8. Li, H.; Cao, F.; Zhao, F.; Yang, Y.; Teng, M.; Wang, C.; Qiu, L. Developmental toxicity, oxidative stress and immunotoxicity induced by three strobilurins (pyraclostrobin, trifloxystrobin and picoxystrobin) in zebrafish embryos. *Chemosphere* **2018**, *207*, 781–790. [CrossRef]
9. Wang, X.; Li, X.; Wang, Y.; Qin, Y.; Yan, B.; Martyniuk, C.J. A comprehensive review of strobilurin fungicide toxicity in aquatic species: Emphasis on mode of action from the zebrafish model. *Environ. Pollut.* **2021**, *275*, 116671. [CrossRef]
10. Pomal, N.C.; Bhatt, K.D.; Kundariya, D.S.; Desai, R.A.; Bhatt, V.; Kongor, A. Calix[4]pyrrole-Grafted Gold Nanoparticles as a Turn-On Fluorescence Sensor for Noxious Fungicide Dimoxystrobin and Their Anti-Cancer Activity against the KB-3-1 Cell Line. *ChemistrySelect* **2023**, *8*, e202204252. [CrossRef]
11. Zhao, Y.; Zhang, H.; Liu, Y.; Lan, Y.; Zhu, J.; Cai, Y.; Guo, F.; Li, F.; Zhang, Y.; Zhang, T.; et al. Evidence of strobilurin fungicides and their metabolites in Dongjiang River ecosystem, southern China: Bioaccumulation and ecological risks. *Sci. Total Environ.* **2024**, *908*, 168427. [CrossRef]
12. European Food Safety Authority (EFSA). Peer review of the pesticide risk assessment of the active substance dimoxystrobin. *EFSA J.* **2023**, *21*, e08329. [CrossRef]
13. Lewis, K.A.; Tzilivakis, J.; Warner, D.J.; Green, A. An international database for pesticide risk assessments and management. *Hum. Ecol. Risk Assess.* **2016**, *22*, 1050–1064. [CrossRef]
14. Pesticide Properties DataBase (PPDB). Dimoxystrobin (Ref: BAS 505F). 2024. Available online: https://sitem.herts.ac.uk/aeru/ppdb/en/Reports/246.htm (accessed on 20 September 2024).
15. CLH Report. Proposal for Harmonised Classification and Labelling Based on Regulation (EC) No 1272/2008 (CLP Regulation), Annex VI, Part 2 Substance Name: Dimoxystrobin. 2019. Available online: https://echa.europa.eu/documents/10162/71711b06-bc63-d700-6553-dd633d93ea8b (accessed on 25 August 2024).

16. Ahmed, A.I.M.; Macirella, R.; Talarico, F.; Curcio, V.; Trotta, G.; Aiello, D.; Gharbi, N.; Mezzasalma, M.; Brunelli, E. Short-term effects of the strobilurin fungicide dimoxystrobin on zebrafish gills: A morpho-functional study. *Chemosphere* **2023**, *333*, 138914. [CrossRef]
17. Ahmed, A.I.M.; Macirella, R.; Talarico, F.; Muoio, M.F.; Mezzasalma, M.; Tronci, V.; Lal, P.; Gharbi, N.; Brunelli, E. Effect of short-term exposure to the strobilurin fungicide dimoxystrobin: Morphofunctional, behavioural and mitochondrial alterations in *Danio rerio* embryos and larvae. *Ecotoxicol. Environ. Saf.* **2024**, *279*, 116493. [CrossRef] [PubMed]
18. Macirella, R.; Guardia, A.; Pellegrino, D.; Bernabò, I.; Tronci, V.; Ebbesson, L.O.; Sesti, S.; Tripepi, S.; Brunelli, E. Effects of two sublethal concentrations of mercury chloride on the morphology and metallothionein activity in the liver of zebrafish (*Danio rerio*). *Int. J. Mol. Sci.* **2016**, *17*, 361. [CrossRef]
19. Popović, N.T.; Čižmek, L.; Babić, S.; Strunjak-Perović, I.; Čož-Rakovac, R. Fish liver damage related to the wastewater treatment plant effluents. *Environ. Sci. Pollut. Res.* **2023**, *30*, 48739–48768. [CrossRef]
20. Araújo, F.G.; Gomes, I.D.; do Nascimento, A.A.; dos Santos, M.A.J.; Sales, A. Histopathological analysis of liver of the catfish *Pimelodus maculatus* in a tropical eutrophic reservoir from Southeastern Brazil. *Acta Sci. Biol. Sci.* **2019**, *41*, 41039. [CrossRef]
21. Rohani, M.F. Pesticides toxicity in fish: Histopathological and hemato-biochemical aspects—A review. *Emerg. Contam.* **2023**, *9*, 100234. [CrossRef]
22. Levina, I.L.; Fedorova, E.A.; Kuznetsova, L.Y.; Zinchuk, O.A. Dynamics of antioxidant protection and detoxication processes affected by strobilurin fungicides in the liver of cyprinids. *Inland Water Biol.* **2012**, *5*, 222–228. [CrossRef]
23. Valenti, M.T.; Marchetto, G.; Mottes, M.; Dalle Carbonare, L. Zebrafish: A suitable tool for the study of cell signaling in bone. *Cells* **2020**, *9*, 1911. [CrossRef]
24. Li, H.; Liu, Y.; Chen, Q.; Jin, L.; Peng, R. Research progress of zebrafish model in aquatic ecotoxicology. *Water* **2023**, *15*, 1735. [CrossRef]
25. Adhish, M.; Manjubala, I. Effectiveness of zebrafish models in understanding human diseases—A review of models. *Heliyon* **2023**, *9*, e14557. [CrossRef]
26. Cortes, L.G.; Marinov, D.; Sanseverino, I.; Cuenca, A.N.; Niegowska, M.; Rodriguez, E.P.; Lettieri, T. *Selection of Substances for the 3rd Watch List Under the Water Framework Directive*; EUR 30297 EN; Publications Office of the European Union: Luxembourg, 2020. [CrossRef]
27. Elizalde-Velázquez, G.A.; Herrera-Vázquez, S.E. Zebrafish as Model Organism in Aquatic Ecotoxicology: Current Trends and Future Perspectives. In *Zebrafish Research—An Ever-Expanding Experimental Model*; Disner, G.D., Ed.; Zebrafish Research; IntechOpen: London, UK, 2023. [CrossRef]
28. Bernet, D.; Schmidt, H.; Meier, W.; Burkhardt-Holm, P.; Wahli, T. Histopathology in fish: Proposal for a protocol to assess aquatic pollution. *J. Fish Dis.* **1999**, *22*, 25–34. [CrossRef]
29. Van Dyk, J.C.; Marchand, M.J.; Smit, N.J.; Pieterse, G.M. A histology-based fish health assessment of four commercially and ecologically important species from the Okavango Delta panhandle, Botswana. *Afr. J. Aquat. Sci.* **2009**, *34*, 273–282. [CrossRef]
30. Sun, Y.; Heng, J.; Liu, F.; Zhang, S.; Liu, P. Isolation and proteomic study of fish liver lipid droplets. *Biophys. Rep.* **2023**, *9*, 120. [CrossRef] [PubMed]
31. Manera, M.; Castaldelli, G.; Fano, E.A.; Giari, L. Perfluorooctanoic acid-induced cellular and subcellular alterations in fish hepatocytes. *Environ. Toxicol. Pharmacol.* **2021**, *81*, 103548. [CrossRef]
32. Flores-Lopes, F.; Correia, M.A.; da Silva, D.M.L. Histological and ultrastructural analysis of *Tilapia rendalli* liver as an environmental assessment tool for Cachoeira River, Bahia, Brazil. *Int. J. Zool. Investig.* **2020**, *6*, 31–48. [CrossRef]
33. Rašković, B.; Poleksić, V. Fish histopathology as biomarker in ecotoxicology. *Trends Fish. Aquat. Anim. Health* **2017**, *27*, 155–181.
34. Huang, X.; Li, Y.; Wang, T.; Liu, H.; Shi, J.; Zhang, X. Evaluation of the oxidative stress status in zebrafish (Danio rerio) liver induced by three typical organic UV filters (BP-4, PABA and PBSA). *Int. J. Environ. Res. Public Health* **2020**, *17*, 651. [CrossRef]
35. Rossi, A.S.; Fantón, N.; Michlig, M.P.; Repetti, M.R.; Cazenave, J. Fish inhabiting rice fields: Bioaccumulation, oxidative stress and neurotoxic effects after pesticides application. *Ecol. Indic.* **2020**, *113*, 106186. [CrossRef]
36. Santana, M.S.; de Melo, G.D.; Sandrini-Neto, L.; Di Domenico, M.; Prodocimo, M.M. A meta-analytic review of fish antioxidant defense and biotransformation systems following pesticide exposure. *Chemosphere* **2022**, *291*, 132730. [CrossRef] [PubMed]
37. Cao, F.; Wu, P.; Huang, L.; Li, H.; Qian, L.; Pang, S.; Qiu, L. Short-term developmental effects and potential mechanisms of azoxystrobin in larval and adult zebrafish (*Danio rerio*). *Aquat. Toxicol.* **2018**, *198*, 129–140. [CrossRef] [PubMed]
38. Cao, F.; Martyniuk, C.J.; Wu, P.; Zhao, F.; Pang, S.; Wang, C.; Qiu, L. Long-term exposure to environmental concentrations of azoxystrobin delays sexual development and alters reproduction in zebrafish (*Danio rerio*). *Environ. Sci. Technol.* **2019**, *53*, 1672–1679. [CrossRef] [PubMed]
39. Organisation for Economic Co-operation and Development (OECD). *OECD Guidelines for the Testing of Chemicals, Fish Embryo Acute Toxicity (FET) Test. Section 2*; OECD Publishing: Paris, France, 2013. [CrossRef]
40. Organisation for Economic Co-operation and Development (OECD). *OECD Guidance Document on Aqueous-Phase Aquatic Toxicity Testing of Difficult Test Chemicals. No. 23*, 2nd ed.; OECD Publishing: Paris, France, 2019. Available online: https://one.oecd.org/document/ENV/JM/MONO(2000)6/REV1/en/pdf (accessed on 30 August 2024).
41. Wallace, C.K.; Bright, L.A.; Marx, J.O.; Andersen, R.P.; Mullins, M.C.; Carty, A.J. Effectiveness of rapid cooling as a method of euthanasia for young zebrafish (*Danio rerio*). *J. Am. Assoc. Lab. Anim. Sci.* **2018**, *57*, 58–63. [PubMed]

42. Macirella, R.; Curcio, V.; Ahmed, A.I.; Talarico, F.; Sesti, S.; Paravani, E.; Odetti, L.; Mezzasalma, M.; Brunelli, E. Morphological and Functional Alterations in Zebrafish (*Danio rerio*) Liver after Exposure to Two Ecologically Relevant Concentrations of Lead. *Fishes* **2023**, *8*, 342. [CrossRef]
43. Macirella, R.; Curcio, V.; Ahmed, A.I.M.; Pellegrino, D.; Brunelli, E. Effect of short-term exposure to low concentration of tebuconazole: Morphological, histometric and functional modifications in *Danio rerio* liver. *Eur. Zool. J.* **2022**, *89*, 331–345. [CrossRef]
44. Livak, K.J.; Schmittgen, T.D. Analysis of relative gene expression data using real-time quantitative PCR and the $2^{-\Delta\Delta CT}$ method. *Methods* **2001**, *25*, 402–408. [CrossRef]
45. Chen, L.; Luo, Y.; Zhang, C.; Liu, X.; Fang, N.; Wang, X.; Zhao, X.; Jiang, J. Trifloxystrobin induced developmental toxicity by disturbing the ABC transporters, carbohydrate and lipid metabolism in adult zebrafish. *Chemosphere* **2024**, *349*, 140747. [CrossRef]
46. Zheng, S.; Yang, Y.; Wen, C.; Liu, W.; Cao, L.; Feng, X.; Chen, J.; Wang, H.; Tang, Y.; Tian, L.; et al. Effects of environmental contaminants in water resources on nonalcoholic fatty liver disease. *Environ. Int.* **2021**, *154*, 106555. [CrossRef]
47. Cao, F.; Zhu, L.; Li, H.; Yu, S.; Wang, C.; Qiu, L. Reproductive toxicity of azoxystrobin to adult zebrafish (*Danio rerio*). *Environ. Pollut.* **2016**, *219*, 1109–1121. [CrossRef]
48. Agamy, E. Histopathological changes in the livers of rabbit fish (*Siganus canaliculatus*) following exposure to crude oil and dispersed oil. *Toxicol. Pathol.* **2012**, *40*, 1128–1140. [CrossRef] [PubMed]
49. Teng, M.; Zhou, Y.; Song, M.; Dong, K.; Chen, X.; Wang, C.; Bi, S.; Zhu, W. Chronic toxic effects of flutolanil on the liver of zebrafish (*Danio rerio*). *Chem. Res. Toxicol.* **2019**, *32*, 995–1001. [CrossRef] [PubMed]
50. Kumar, M.; Mishra, A.; Verma, A.; Jain, A.; Khan, A.A.; Dwivedi, S.; Trivedi, S.P. Assessment of oxidative stress, genotoxicity, and histopathological alterations in freshwater food fish *Channa punctatus* exposed to fungicide, Mancozeb. *J. Appl. Biol.* **2024**, *12*, 159–164. [CrossRef]
51. Shan, Z.; Ju, C. Hepatic macrophages in liver injury. *Front. Immunol.* **2020**, *11*, 322. [CrossRef]
52. Bjørgen, H.; Koppang, E.O. The melano-macrophage: The black leukocyte of fish immunity. *Fish Shellfish Immunol.* **2024**, *148*, 109523. [CrossRef]
53. Oliveira, S.E.; Costa, P.M.; Nascimento, S.B.; Castro, W.V.; de Azambuja Ribeiro, R.I.M.; Santos, H.B.; Thomé, R.G. Atrazine promotes immunomodulation by melanomacrophage centre alterations in spleen and vascular disorders in gills from *Oreochromis niloticus*. *Aquat. Toxicol.* **2018**, *202*, 57–64. [CrossRef]
54. Hamed, M.; Said, R.E.; Soliman, H.A.; Osman, A.G.; Martyniuk, C.J. Immunotoxicological, histopathological, and ultrastructural effects of waterborne pyrogallol exposure on African catfish (*Clarias gariepinus*). *Chemosphere* **2024**, *349*, 140792. [CrossRef]
55. Sayed, A.E.D.H.; Abd-Elkareem, M.; Abou Khalil, N.S. Immunotoxic effects of 4-nonylphenol on *Clarias gariepinus*: Cytopathological changes in hepatic melanomacrophages. *Aquat. Toxicol.* **2019**, *207*, 83–90. [CrossRef]
56. Narra, M.R.; Rajender, K.; Reddy, R.R.; Rao, J.V.; Begum, G. The role of vitamin C as antioxidant in protection of biochemical and haematological stress induced by chlorpyrifos in freshwater fish *Clarias batrachus*. *Chemosphere* **2015**, *132*, 172–178. [CrossRef]
57. Singh, D.P.; Kumar, A. Changes in liver glycogen contents in fresh water fishes due to cobalt toxicity. *J. Exp. Zool. India* **2013**, *16*, 519–521.
58. Roy George, K.; Malini, N.A.; Rani, G.S. Biochemical changes in liver and muscle of the cichlid, *Oreochromis mossambicus* (Peters, 1852) exposed to sub-lethal concentration of mercuric chloride. *Indian J. Fish.* **2012**, *59*, 147–152.
59. Banaee, M.; Sagvand, S.; Sureda, A.; Amini, M.; Haghi, B.N.; Sopjani, M.; Faggio, C. Evaluation of single and combined effects of mancozeb and metalaxyl on the transcriptional and biochemical response of zebrafish (*Danio rerio*). *Comp. Biochem. Physiol. Part C Toxicol.* **2023**, *268*, 109597. [CrossRef]
60. Schwaiger, J.; Fent, K.; Stecher, H.; Ferling, H.; Negele, R.D. Effects of sublethal concentrations of triphenyltinacetate on rainbow trout (*Oncorhynchus mykiss*). *Arch. Environ. Contam. Toxicol.* **1996**, *30*, 327–334. [CrossRef]
61. Sharma, R.; Jindal, R. Assessment of cypermethrin induced hepatic toxicity in *Catla catla*: A multiple biomarker approach. *Environ. Res.* **2020**, *184*, 109359. [CrossRef] [PubMed]
62. Vani, G.; Veeraiah, K.; Kumar, M.V.; Parveen, S.; GRao, D.P. Biochemical changes induced by Cartap hydrochloride (50% SP), carbamate insecticide in freshwater fish *Cirrhinus mrigala* (Hamilton, 1822). *Nat. Environ. Pollut. Technol.* **2020**, *19*, 1821–1828. [CrossRef]
63. Yadavrao, W.S. Confidor and Bavistin induced effects on total glycogen content in liver and gonads of snakeheaded fish, *Channa gachua*. *Pharm. Innov.* **2017**, *6*, 41–43.
64. Georgieva, E.; Kovacheva, E.; Yancheva, V.; Velcheva, I.; Hrischev, P.; Atanassova, P.; Tomov, S.; Stoyanova, S. Pesticides induce fatty degeneration in liver of *Cyprinus carpio* (Linnaeus 1758) after acute exposure. *Ecol. Balk.* **2023**, *15*, 77–82.
65. Stoyanova, S.; Georgieva, E.; Velcheva, I.; Yancheva, V. Histochemical Alterations in Bighead Carp (*Hypophthalmichthys nobilis Richardson*, 1845) Liver Under Two Pesticides Exposure: A Comparative Study. *Ecol. Balk.* **2019**, *11*, 63–71.
66. Sun, L.; Li, J.; Zuo, Z.; Chen, M.; Wang, C. Chronic exposure to paclobutrazol causes hepatic steatosis in male rockfish *Sebastiscus marmoratus* and the mechanism involved. *Aquat. Toxicol.* **2013**, *126*, 148–153. [CrossRef]
67. Arellano, J.M.; Storch, V.; Sarasquete, C. Histological changes and copper accumulation in liver and gills of the Senegales sole, *Solea senegalensis*. *Ecotoxicol. Environ. Saf.* **1999**, *44*, 62–72. [CrossRef]
68. Bonifacio, A.F.; Hued, A.C. Single and joint effects of chronic exposure to chlorpyrifos and glyphosate based pesticides on structural biomarkers in *Cnesterodon decemmaculatus*. *Chemosphere* **2019**, *236*, 124311. [CrossRef] [PubMed]

69. Bleier, L.; Dröse, S. Superoxide generation by complex III: From mechanistic rationales to functional consequences. *Biochim. Biophys. Acta Bioenerg.* **2013**, *1827*, 1320–1331. [CrossRef] [PubMed]
70. Dröse, S.; Brandt, U. The mechanism of mitochondrial superoxide production by the cytochrome *bc1* complex. *J. Biol. Chem.* **2008**, *283*, 21649–21654. [CrossRef] [PubMed]
71. Jena, A.B.; Samal, R.R.; Bhol, N.K.; Duttaroy, A.K. Cellular Red-Ox system in health and disease: The latest update. *Biomed. Pharmacother.* **2023**, *162*, 114606. [CrossRef]
72. Jomova, K.; Alomar, S.Y.; Alwasel, S.H.; Nepovimova, E.; Kuca, K.; Valko, M. Several lines of antioxidant defense against oxidative stress: Antioxidant enzymes, nanomaterials with multiple enzyme-mimicking activities, and low-molecular-weight antioxidants. *Arch. Toxicol.* **2024**, *98*, 1323–1367. [CrossRef]
73. Fang, N.; Zhang, C.; Hu, H.; Li, Y.; Wang, X.; Zhao, X.; Jiang, J. Histology and metabonomics reveal the toxic effects of kresoxim-methyl on adult zebrafish. *Chemosphere* **2022**, *309*, 136739. [CrossRef]
74. Jia, W.; Mao, L.; Zhang, L.; Zhang, Y.; Jiang, H. Effects of two strobilurins (azoxystrobin and picoxystrobin) on embryonic development and enzyme activities in juveniles and adult fish livers of zebrafish (*Danio rerio*). *Chemosphere* **2018**, *207*, 573–580. [CrossRef]
75. Mao, L.; Jia, W.; Zhang, L.; Zhang, Y.; Zhu, L.; Sial, M.U.; Jiang, H. Embryonic development and oxidative stress effects in the larvae and adult fish livers of zebrafish (*Danio rerio*) exposed to the strobilurin fungicides, kresoxim-methyl and pyraclostrobin. *Sci. Total Environ.* **2020**, *729*, 139031. [CrossRef]
76. Zhang, C.; Zhou, T.; Wang, J.; Zhang, S.; Zhu, L.; Du, Z.; Wang, J. Acute and chronic toxic effects of fluoxastrobin on zebrafish (*Danio rerio*). *Sci. Total Environ.* **2018**, *610*, 769–775. [CrossRef]
77. Crupkin, A.C.; Fulvi, A.B.; Iturburu, F.G.; Medici, S.; Mendieta, J.; Panzeri, A.M.; Menone, M.L. Evaluation of hematological parameters, oxidative stress and DNA damage in the cichlid *Australoheros facetus* exposed to the fungicide azoxystrobin. *Ecotoxicol. Environ. Saf.* **2021**, *207*, 111286. [CrossRef]
78. Zhao, H.; Zhang, J.; Rajeshkumar, S.; Feng, Y.; Liu, Y.; Li, X.; Zhang, B. Hepatopancreas toxicity and immunotoxicity of a fungicide, pyraclostrobin, on common carp. *Comp. Biochem. Physiol. Part C Toxicol.* **2022**, *262*, 109445. [CrossRef] [PubMed]
79. Zhang, C.; Wang, J.; Zhang, S.; Zhu, L.; Du, Z.; Wang, J. Acute and subchronic toxicity of pyraclostrobin in zebrafish (*Danio rerio*). *Chemosphere* **2017**, *188*, 510–516. [CrossRef]
80. Liu, L.; Jiang, C.; Wu, Z.Q.; Gong, Y.X.; Wang, G.X. Toxic effects of three strobilurins (trifloxystrobin, azoxystrobin and kresoxim-methyl) on mRNA expression and antioxidant enzymes in grass carp (*Ctenopharyngodon idella*) juveniles. *Ecotoxicol. Environ. Saf.* **2013**, *98*, 297–302. [CrossRef]
81. Casalino, E.; Calzaretti, G.; Sblano, C.; Landriscina, C. Molecular inhibitory mechanisms of antioxidant enzymes in rat liver and kidney by cadmium. *Toxicology* **2002**, *179*, 37–50. [CrossRef] [PubMed]
82. Ghelichpour, M.; Mirghaed, A.T.; Hoseinifar, S.H.; Khalili, M.; Yousefi, M.; Van Doan, H.; Perez-Jimenez, A. Expression of immune, antioxidant and stress related genes in different organs of common carp exposed to indoxacarb. *Aquat. Toxicol.* **2019**, *208*, 208–216. [CrossRef] [PubMed]
83. Rossi, A.S.; Michlig, M.P.; Repetti, M.R.; Cazenave, J. Single and joint toxicity of azoxystrobin and cyproconazole to Prochilodus lineatus: Bioconcentration and biochemical responses. *Sci. Total Environ.* **2024**, *907*, 167992. [CrossRef]
84. Tabassum, H.; Dawood, A.Q.; Sharma, P.; Khan, J.; Raisuddin, S.; Parvez, S. Multi-organ toxicological impact of fungicide propiconazole on biochemical and histological profile of freshwater fish *Channa punctata* Bloch. *Ecol. Indic.* **2016**, *63*, 359–365. [CrossRef]
85. Ahmad, I.; Pacheco, M.; Santos, M.A. Enzymatic and nonenzymatic antioxidants as an adaptation to phagocyte-induced damage in *Anguilla anguilla* L. following in situ harbor water exposure. *Ecotoxicol. Environ. Saf.* **2004**, *57*, 290–302. [CrossRef]
86. Isik, I.; Celik, I. Acute effects of methyl parathion and diazinon as inducers for oxidative stress on certain biomarkers in various tissues of rainbowtrout (*Oncorhynchus mykiss*). *Pestic. Biochem. Physiol.* **2008**, *92*, 38–42. [CrossRef]

Disclaimer/Publisher's Note: The statements, opinions and data contained in all publications are solely those of the individual author(s) and contributor(s) and not of MDPI and/or the editor(s). MDPI and/or the editor(s) disclaim responsibility for any injury to people or property resulting from any ideas, methods, instructions or products referred to in the content.